RSC Advances

PAPER

View Article Online
View Journal | View Issue

Cite this: *RSC Adv.*, 2019, **9**, 34389

Synthesis and characterization of a novel, pH-responsive, bola-based dynamic crosslinked fracturing fluid

Juan Du, *[a] Kun Xiang,[a] Liqiang Zhao,*[a] Xitang Lan,[b] Pingli Liu[a] and Yue Liu[a]

Received 16th April 2019
Accepted 13th August 2019

DOI: 10.1039/c9ra02853f

rsc.li/rsc-advances

Fracturing fluids are important media for hydraulic fracturing. Typically, the fluids are gelled using a polymeric gelling agent. Technological improvements over the years have focused primarily on improving the rheological performance, thermal stability, and the clean-up of crosslinked gels. In this study, novel supramolecular assembly of a low-damage fracturing fluid combining an ionic polymer gel (hydroxypropyl trimethylammonium chloride guar-cationic guar) and a bola surfactant fluid (bola carboxylate polypropylene glycol) is carried out and it is reported to have improved properties and special characteristics due to the synergistic effects of the dual systems, which are different from those of polymer gels and surfactant fluids. The viscosity of the fracturing fluid shows a sudden increase upon an increase in temperature and excellent self-assembly recovery after shearing. The fracturing fluid exhibits pH-responsive viscosity changes and low permeability impairment, due to the formation of a network structure and supramolecular microspheres at different pH values.

1 Introduction

In recent years, with the growing demand for energy in the world, the use of unconventional oil and gas sources, such as tight oil and gas,[1–3] coalbed methane,[4–6] shale gas and so on, has risen rapidly.[7–9] Hydraulic fracturing is the most effective technology to enhance the productivity of oil and gas wells, which works by creating a highly conductive path. The traditional cross-linked polymer residues left in the fractures significantly damage the reservoir conductivity after fracturing. In order to reduce the damage to reservoir permeability by polymer residues, a viscoelastic surfactant (VES) fluid has been widely used for fracturing over the past 20 years.[10–12] The VES is a supramolecular body formed by hydrophobic action of surfactant molecules contributed to stabilizing the viscosity of fracturing fluids, causing that it has larger dosage and lower viscosity than crosslinked polymer fracturing fluid. Thus, it is necessary to develop an alternative gel system with improved viscosity stability, proppant suspension, low-damage, and fluid loss properties.

Surfactant–polymers, based on non-covalent forces, as mechanically strong and tough hydrogels, are widely used in the enhanced oil recovery (EOR) process,[13,14] but very few studies have been carried out on their application as fracturing gels.[15,16] Upon an increase in the concentration of sodium dodecyl sulfate (SDS) from 0 to 0.043%, the apparent viscosity of cationic guar solutions with SDS can be increased by nearly 3 orders of magnitude.[17] The addition of ionic surfactants is an effective way to obtain stable alginic acid/alumina gels.[18] The double network approach offers improved potential for the future application of microgels in high load environments.[19] GLDA (*N*,*N*-dicarboxymethyl glutamic acid tetrasodium salt) is a surface-active fluid that reduces interfacial tension and eliminates the water-blockage effect, which combined with a polymer in fracturing fluid can withstand a formation temperature of up to 300 °F and is stable for about 6 h under high shearing rates (511 s^{-1}).[20] Carboxymethyl hydroxypropyl guar gum (CMHPG)–sodium oleate microemulsion gels show improved rheology with higher thermal stability, and better clean-up properties with less residues, as compared with their individual components.[15] A HMPAM (Hydrophobic Modified Polyacrylamide)-VES fracturing fluid possesses favorable temperature tolerance, shearing resistance, and proppant suspension ability due to its multiple supermolecular behavior and high viscoelasticity, and a complex supermolecular gel is achieved through the effects of weak physical attractive forces.[12] In a fiber-VES fracturing fluid, the fibers strengthen the mechanical properties of the network structure formed by the fibers in VES, which improves the rheological properties of the fluid.[21]

The stability of the EOR and fracturing solution can be boosted due to the synergistic effect of the hydrophobic surfactant and polymer.[12,15,22] However, the hydrophobic association effect contributes to the generation of surfactant micelles instead of a favorable dispersed system with the

[a]*School of Petroleum and Natural Gas Engineering, State Key Lab, Southwest Petroleum University, Chengdu, Sichuan 610500, People's Republic of China. E-mail: dujuanswpu@163.com; zhaolq@vip.163.com*

[b]*CNOOC China Co. Ltd, Tianjin branch, Tianjin 300000, People's Republic of China*

polymer. In addition, the dissolution capacity of the surfactant indeed decreases with an increase in the length of the carbon chain.[23] Based on pioneering work in this field, it is believed that the viscoelastic and low-damage properties of a fracturing fluid can be improved by the interaction between ionic bola-type supramolecules and an aqueous polymer solution. With this in mind, a new type of fracturing fluid with low-damage, viscoelastic and self-assembly properties, named BSP, was designed in our group. The BSP fracturing fluid is a hydrogel formed through the synergistic effect of cationic guar (CG) and a bola carboxylate surfactant (BS). There are three reasons for its stability. First of all, supramolecular electrostatic bridges between BS and CG groups are formed in solution. What is more, the dynamic crosslinking action of the bola surfactant makes the system repairable. Finally, the long-chain hydrophobic structures of BS and CG intertwine, further increasing the binding forces.[15] The reason for it being a low-damage fracturing fluid is that a decrease of the pH leads to the destruction of the structure of the BS and CG electrostatic bridges network after fracturing, reducing the viscosity of BSP to realize low-damage fracturing. In addition, the stability of the BSP system is achieved *via* a supramolecular self-assembly method based on pH response. Compared to conventional high-valence metal crosslinking, the use of BSP results in low damage to reservoirs and compared to conventional VES, BSP uses fewer agents.

2 Experimental section

2.1 Materials

CG ($M_W = 2.5 \times 10^5$), proppant (20 to 40 mesh ceramsite) and artificial core (diameter of 25 mm, length of 60 mm, and permeability of 30 mD) were purchased from Chengdu Acidizing Petroleum Technology Development Co., Ltd. Polypropylene glycol (PPG2000), sodium chloroacetate ($C_2H_2ClNaO_2$), ethanol, KCl, NaCl, $MgCl_2$, $CaCl_2$, HCl and NaOH were all obtained from Chengdu Kelong Chemical Reagents Corporation (Chendu, P. R. China), and were of analytical reagent grade. Deionized (DI) water was obtained from a water purification system. All chemicals and reagents were utilized without further purification.

2.2 Preparation of BSP

The BSP fracturing fluid is formed by the synergistic effect of CG and BS, which is both a physical and chemical effect. CG is a dispersed polymer chain in aqueous solution, and BS is either dispersed or in the form of aggregated molecular micelles in aqueous solution. The CG molecule chain is positively charged, while the BS molecule is negatively charged. When they meet under certain conditions, a spaced network structure is formed through electrostatic bridges. The BSP fracturing fluid preparation steps include adjusting the pH value of the aqueous solution to 4–6 with HCl, making CG and BS easy to disperse; then slowly adding the CG to the aqueous solution and stirring evenly; then allowing the CG aqueous solution to stand for more than 24 h, waiting for the CG molecules to stretch; the BS is added into the CG solution and stirred evenly; and then the pH is adjusted to 10 with NaOH. In fracturing engineering applications, solutions that mix NaOH and BS, CG aqueous solution and BS aqueous solution together in the wellbore *via* a three-way pipeline can be injected into the formation.

2.3 Synthesis of BS

$C_2H_2ClNaO_2$, PPG and NaOH ($\omega_{C_2H_2ClNaO_2} = 10\%$, $\omega_{PPG} = 88\%$, $\omega_{NaOH} = 2\%$) were added into a four-neck round-bottom flask equipped with a stirrer, thermometer, and suction pipe, which was then immersed in a 70 °C water bath, violent stirring, under negative pressure for 6 h. After completion of the reaction, a dark brown viscous liquid was obtained. Subsequently, it was purified to remove any remaining $C_2H_2ClNaO_2$ and NaCl by filtration with ethanol. Finally, it was dried in a vacuum desiccator and stored for further use. The chemical reaction process is shown in Scheme 1 and images of the BS product are shown in Fig. 1. The BS aqueous solution is clear at 20 °C, but turns milky white at 65 °C, which indicates that heat improves the activity of BS.

3 Experimental tests

3.1 Structural characterization of BS

The ^1H NMR spectrum of BS in $CDCl_3$ was recorded on a Bruker Advance 400 MHz spectrometer. The infrared spectrum of BS was recorded using a WQ-520 (Shanghai, China) Fourier-transform infrared (FTIR) spectrometer at a resolution of 4 cm^{-1}, where the data was collected over a wavelength of 400–4000 cm^{-1} for 64 scans.

3.2 Apparent viscosity and rheological measurements

Apparent viscosity was measured using a NDJ-8S viscometer (Shanghai, China) with various concentrations and temperatures, used to optimize the concentration and pH value of the BSP system. The pH of the fracturing fluid was determined by a PHS-25 meter (Rex Electric Chemical, China).

The dynamic rheological properties were determined using a rotary rheometer (MCR302 Anton Paar GmbH Austria). The effects of temperature (20 to 110 °C), shear time (5 to 95 min), shear rate (0 to 1000 s^{-1}), and pressure (0.1 to 45 MPa) on the viscosity were investigated. Rheological measurement results can be used to determine the stability of the BSP system in fracturing, for example, the influence of rock shear, high pressure in a reservoir and sand-carrying shear on the viscoelasticity of the fracturing fluid. The shear recovery and strain recovery were measured by a rheometer. The degree of recovery of the viscosity of the BSP system under different shear speeds (20 to 170 s^{-1}) and the degree of the recovery of the BSP system modulus under different stresses (1% to 300% yield stress) were measured, and used to judge the recovery effect of the BSP system structure under high speed shear and high pressure.

3.3 Application simulation of BSP fracturing fluid

As the primary property of fracturing fluids, good suspension ability is an effective way to ensure transport of the proppant to

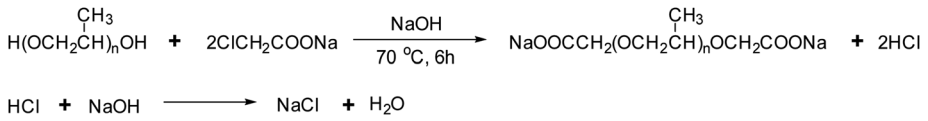

Scheme 1 Synthesis of the BS.

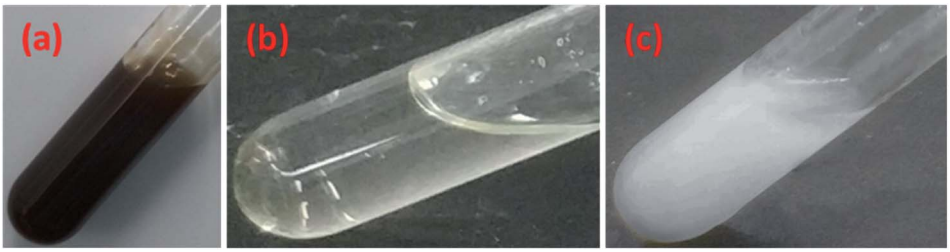

Fig. 1 BS solution. (a) Purified. (b) 1% BS (20 °C). (c) 1% BS (65 °C).

the fracture formations. BSP fracturing fluid with 30% proppant was poured into a measuring cylinder, and then the proppant settling velocity was recorded at different times.

Low permeability damage has been the research direction of fracturing fluids. The damage characteristics of the BSP fracturing fluid were tested by carrying out core flooding experiments. During the initial state, the permeability, K_1, of the brine flooding core was tested, and then the permeability, K_2, of brine flooding core was tested after saturating the core with BSP fracturing fluid. The damage rate was determined using $(K_1 - K_2)/K_1$.

3.4 Microstructure of the BSP

Cryo-scanning electron microscopy (Cryo-SEM) was used to investigate the microstructure of the BSP fracturing fluid (pH = 10, 7) and BS solution. SEM measurements were performed using a Quanta 450 microscope (FEI, America), where the fluid samples were frozen at −165 °C before scanning.

4 Results and discussion

4.1 Structural characterization of BS

The structure of this compound was characterized using ^{1}H NMR and FT-IR spectroscopies. Although the grafted methylene group could not be clearly detected due to its small proton proportion, the proton fraction in the ^{1}H NMR spectrum (as shown in Fig. 2) indisputably illustrates the presence of PPG structural units. After carefully comparing the structure of PPG and the desired product, an FT-IR spectrum (as shown in Fig. 3) was recorded to further identify this compound. IR peaks for carboxyl groups appeared at about 1600 cm^{-1}, demonstrating the successful synthesis of the bola product.

4.2 Concentration and pH optimization of the BSP

Apparent viscosity testing is a simple way to analyze the influences of different additives on a fracturing fluid. BSP is a supramolecular weak gel composed of bola surfactant and ionic polymer, the viscosity of the gum gels reaches its highest value when the pH ranges from 9 to 11.[24,25] The effect of the concentration ratio of BS and CG on the apparent viscosity of BSP was tested, at pH = 10.

The apparent viscosities of aqueous solutions of BS and CG are presented in Fig. 4. When the concentration of BS increases from 0 to 4%, the viscosity of the solution increases from 1 to 2.7 mPa s, which shows that the apparent viscosity of the BS solution increases along with an increasing concentration of BS, but very slowly, and that the bola surfactant cannot form a network structure and can only be dispersed in solution. When the concentration of CG increases from 0 to 0.3%, the viscosity of the solution increases from 1 to 45 mPa s. The apparent viscosity of the CG solution increases exponentially along with an increasing concentration of CG, consistent with the Huggins equation, which describes the relationship between polymer viscosity and concentration.[26–28]

$$\eta_{sp} = \frac{\eta - \eta_s}{\eta_s} \quad (1)$$

$$\eta_{sp} = [\eta]c + K_1[\eta]^2c^2 + K_2[\eta]^3c^3 \quad (2)$$

where η_{sp} is the specific viscosity (mPa s), η is the viscosity of the polymer solution (mPa s), η_s is the viscosity of the solvent (mPa s), c is the concentration of the polymer solution (mg L^{-1}), and K is the Huggins constant, with K values ranging from 0.3 to 0.5.

The Huggins equation shows that the viscosity of a fracturing fluid can be enhanced by increasing the concentration of the polymer, but also has an impact on the permeability impairment. In this study, the interaction of the bola surfactant and the ionic polymer increases the viscosity of the fracturing fluid with low damage to reservoir permeability.

The effect of different concentration ratios of BS and CG on the apparent viscosity of BSP shows a similar shape to a peak (Fig. 5 and Table 1), namely, increasing at first and then decreasing. Fig. 5 demonstrates that when the concentration ratio of BS to CG is less than 1, the viscosity of BSP is increased

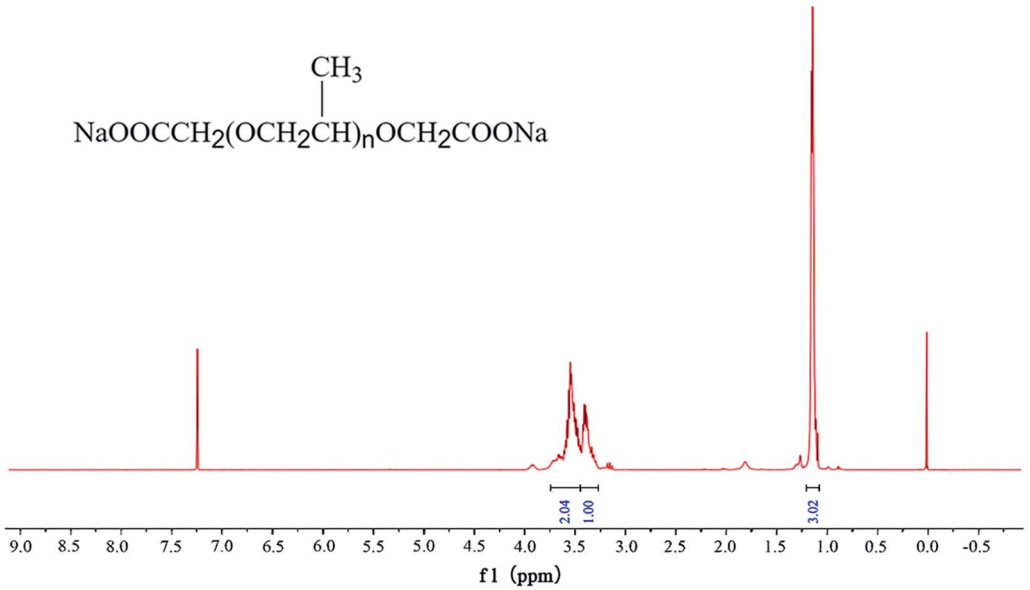

Fig. 2 ^{1}H NMR spectrum of BS.

with the increase in the concentration of the bola. When the concentration ratio of BS to CG is more than 1, the viscosity of BSP is decreased with the increase in the concentration of bola, and the higher the total concentration of the system, the faster the viscosity decreases. When there is an excessive concentration of bola, micelles of the bola surfactant are formed, as shown in Fig. 1(c), resulting in reduced bridging between the bola surfactant molecules and ionic polymer, which is similar to how surfactants form micelles.[29,30]

Fig. 5 shows that when the concentration ratio of BS to CG is constant, the apparent viscosity of BSP improves rapidly with an increase in the CG concentration. Fig. 4 and 5 show that the concentration of CG is the main controlling factor of the apparent viscosity of the BSP fracturing fluid. When the same quantity of BS was added into the CG solution, the viscosity of the system was improved by more than 10 times, which indicates that the BS is the main controlling factor behind BSP forming a network structure. The surfactant can increase the viscosity of the CG solution by up to three times.[31] Conventional surfactant in the right proportions with cosurfactant and polymer forms a stabilized microemulsion with increased viscosity.[15] The double-headed structure of the bola surfactant

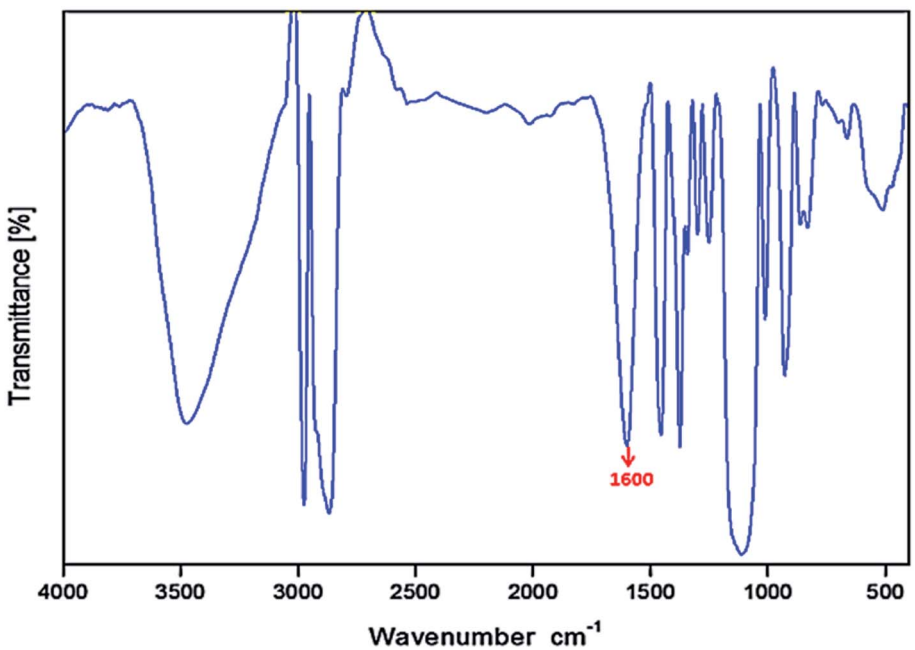

Fig. 3 FT-IR spectrum of BS.

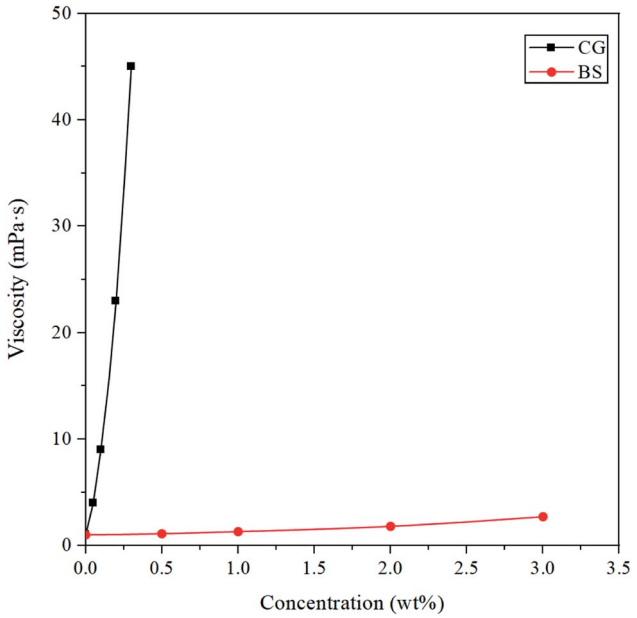

Fig. 4 The apparent viscosity of aqueous solutions of BS and CG (25 °C), 100 s^{-1}.

can form a "hand-in-hand" network with the ionic polymer gel to improve the viscosity of the BSP system. The essence of stabilizing the viscosity of the fracturing fluid is the network structure of the polymer.[32,33]

The effect of pH on the apparent viscosity of the BSP was investigated. In Fig. 6, the four curves show that the value of the pH has a great influence on the apparent viscosity of BSP. The apparent viscosity of BSP shows a small hump-shaped trend with an increase in the pH value. Curve 1 (black) shows that when the pH decreases from 10 to 6, the apparent viscosity of BSP reduces from 545 to 19 mPa s, and at pH = 7–8, the apparent viscosity of BSP reduces rapidly by about 10 times. When the pH increases from 10 to 13, the apparent viscosity of BSP reduces from 545 to 446 mPa s, and the apparent viscosity of BSP decreases by about 20%. For curves 2 (red), 3 (blue) and 4 (green), there are the same variation rules. Fig. 6 shows that the apparent viscosity change of the BSP fracturing fluid is affected by pH, and that during the change from an alkaline to acidic environment, the viscosity of BSP changes greatly. The value of pH also affects the viscosity of boron-crosslinked guar gum fracturing fluid, as when the value of pH decreases from 10 to 7, the viscosity of the boron-crosslinked guar gum fracturing fluid reduces from 280 to 140 mPa s,[25] a reduction of 50%. When the pH decreases from 10 to 7, the BSP fracturing fluid viscosity of curve 2 reduces from 328 to 16 mPa s, a reduction of 95%. The decrease in pH influences the extension of the polymer chains without destroying the coordination bonds between the boron and guar gum. The value of pH affects the electrostatic interactions between BS and CG, and changes the viscosity of the BSP fracturing fluid. There have been many research studies on conventional surfactant–polymer gels, and these studies have shown that conventional surfactants form emulsions with polymers to stabilize and increase gel viscosity.[34,35] Conventional surfactants can improve the viscosity of borate-crosslinked HPGG by more than 10%.[36] There have been many research studies on pH-responsive gels involving a surfactant and polymer. For example, pH-responsive gels have been prepared using sodium oleate and gelatin gel.[37] In another example, drug release has been controlled by adjusting the gel strength through pH response.[38]

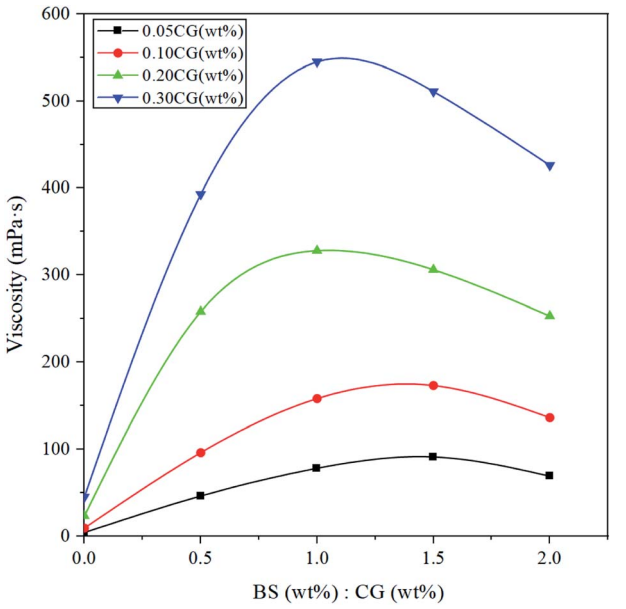

Fig. 5 The apparent viscosity of BSP with different concentration ratios of BS and CG (25 °C), 100 s^{-1}.

A diagram of the mechanism showing the stability and viscosity changes of BSP is illustrated in Fig. 7, which shows that the viscosity of BSP increases because of the network structure cross-linking of the bola surfactant and ionic polymer. The viscosity of the BSP system is the highest at pH = 9–11, while the viscosity of the BSP system decreases rapidly at pH < 8, due to the value of the pH affecting the charge of the bola surfactant.

4.3 Measurement of the rheological properties of the BSP

The temperature and shearing rate resistance are the most important indexes by which to evaluate the suspension and fracturing capacity of a fracturing fluid system.[39–41] Fig. 8 presents the results of temperature stability testing of three systems with different amounts of BS and CG, where the fluid was tested at a shearing rate of 170 s^{-1} and varying the temperature from 20 to 109 °C, with the shearing lasting for 1 min at each temperature point. It was found that the viscosities of the three systems decrease with an increase in the temperature, and that the viscosities of the three systems show a sudden increase from 55 to 70 °C, giving the appearance of a hump, as the viscosities then decrease rapidly when the temperature is higher than 70 °C, and slowly when the temperature is higher than 80 °C. This behavior is completely different from that of metal-crosslinked polymer and VES fracturing fluid systems, the viscosities of which gradually decrease with an increase in the temperature.[22,42,43] Molecular thermodynamic movement is the

Table 1 The apparent viscosity of BSP with different concentration ratios of BS and CG (25 °C), 100 s^{-1}

CG (wt%) = 0.05		CG (wt%) = 0.1		CG (wt%) = 0.2		CG (wt%) = 0.3		BS (wt%) : CG (wt%)
BS (wt%)	Viscosity (mPa s)	BS (wt%)	Viscosity (mPa s)	BS (wt%)	Viscosity (mPa s)	BS (wt%)	Viscosity (mPa s)	
0	4	0	9	0	23	0	45	0
0.025	46	0.05	96	0.1	258	0.15	393	0.5
0.05	78	0.1	158	0.2	328	0.3	545	1
0.075	91	0.15	173	0.2	306	0.45	511	1.5
0.1	69	0.2	136	0.4	253	0.6	426	2

cause of the decrease in the viscosity of metal-crosslinked polymer and VES fracturing fluid systems. However, there are so many chemical forces in the BS and CG system that the viscosity of the system shows a special thermal response. Between 55 and 70 °C, it may be that the thermal effect enhances the thermal mobility of BS, which in effect accentuates the molecular network alignment of the BSP system. This leads to other temperature independent micelle aggregates, hence accentuating the shear and thermal stability.[44,45] With an increase in the temperature, the thermal effect of molecules becomes stronger and perturbs the network alignments,[44,45] reducing the viscosity of the system.

Fig. 9 shows the effect of shearing time on the apparent viscosity of BSP systems, where the temperature of the fluid systems is 65 °C and the shear rate was kept at 170 s^{-1}. The variation in the viscosities of the three BSP systems is quite similar to that of the slightly increasing tendency of the three curves with an increase in the shearing time, which indicates that the BSP systems have good shearing resistance. This is different from conventional metal-crosslinked polymer fracturing fluids, the viscosities of which decrease slightly with an increase in the shearing time. The viscosities of the BSP systems are well maintained with shearing time, similar to the VES fracturing fluid, because shearing does not destroy the dynamic-linking effect between the surfactant and polymer. After 90 minutes, the viscosities of the three systems in the experiment are respectively greater than 90, 260 and 480 mPa s, which means that the fluid systems maintain good performance in suspending proppants at 65 °C.

The easiest way to judge whether a fluid is Newtonian or non-Newtonian is by testing the effect of the shear rate on the fluid viscosity. Fig. 10 shows the relationship between the viscosity and shear rate of the BSP systems, where the fluids were tested at 65 °C with the shear rate ranging from 0 to 1000 s^{-1}, measuring each shear rate level for 90 s. It can be seen that the viscosities of the three BSP systems decrease with an increase in the shear rate, indicating that the BSP systems are non-Newtonian fluids. Moreover, the higher the concentration of agents in the system, the stronger the non-Newtonian performance. These results indicate that the viscosities of the BSP systems can be stabilized *via* the intertwining of agents in the system, contributing towards reducing fluid leakage and increasing the sand carrying capacity of the fracturing fluids during fracturing operation.

Fig. 8, 9 and 10 show the rheological property measurements of the three BSP systems. The three systems show the same trend in viscosity change, and the viscosities of the systems increase with an increase in the BS and CG concentrations. Therefore, the concentration of the system can be optimized according to the reservoir conditions in the application, when the reservoir pressure is lower than 45 MPa, BSP can be preferably 0.5% BS + 0.5% CG or lower. For unconventional reservoirs, such as coalbed methane, the reduction in the concentration of BSP system is conducive to decreasing the damage of reservoir permeability caused by the fracturing fluid.

Fig. 11 shows the stability tests of continuous shearing at 25, 65, 90 and 120 °C, at a shearing rate of 170 s^{-1}, where the shearing lasts for 30 min at each temperature point. It can be seen that the viscosity value curves of the BSP fracturing fluid decrease with an increase in temperature from 25 to 120 °C. The viscosity value of the BSP decreased by about 120 mPa s from 25 to 65 °C, about 200 mPa s from 65 to 90 °C, and about 80 mPa s from 90 to 120 °C. Fig. 8 shows a hump shape in the BSP viscosity values at 65 °C, and taking polymer fracturing fluid as an example,[46,47] the viscosity of the BSP system shows a smaller decrease on going from surface (25 °C) to reservoir

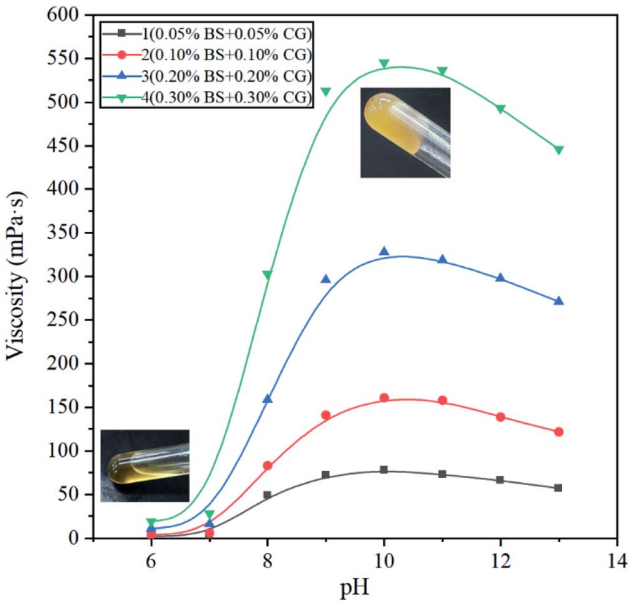

Fig. 6 Effect of pH on the apparent viscosity of the BSP (25 °C), 100 s^{-1}.

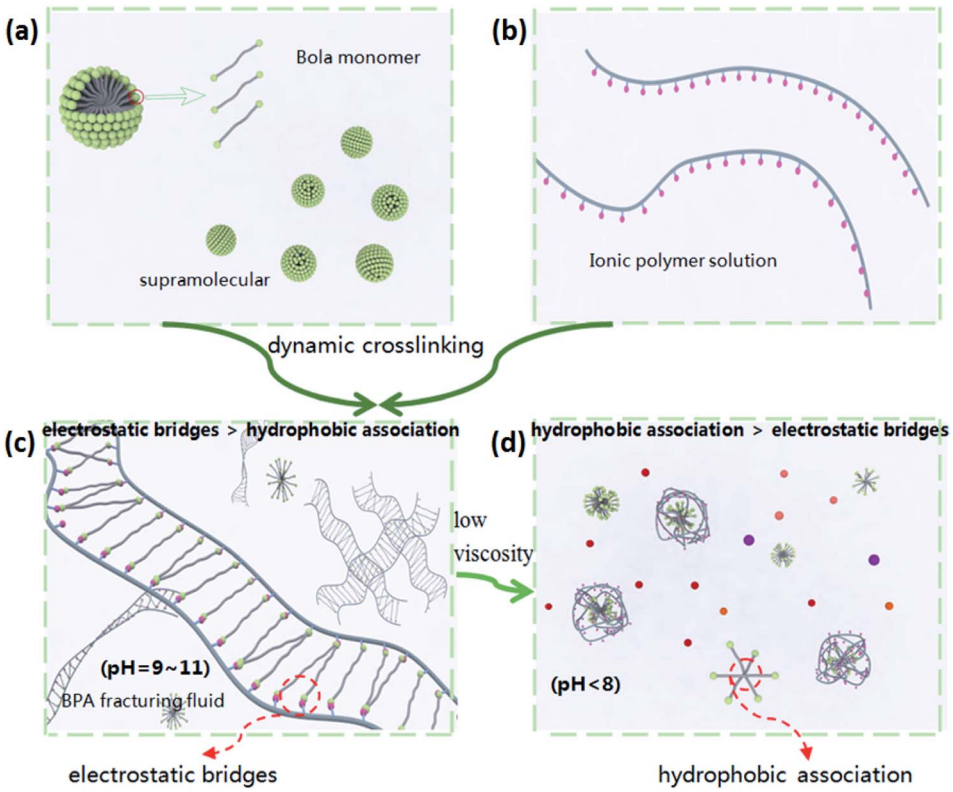

Fig. 7 Diagram of the mechanism of the stability and low-damage properties of the BSP *via* dynamic crosslinking and pH-response.

conditions (65 °C). The viscosity of the BSP system largely decreases from 65 to 120 °C, where the viscosity of the BSP system is greater than 100 mPa s, which indicates that the BSP fracturing fluid maintains a better performance after continuous shearing at 90 and 120 °C.

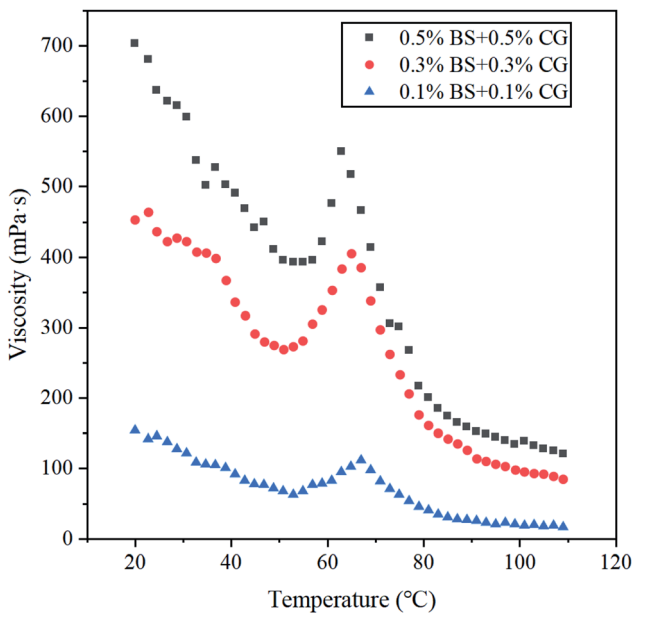

Fig. 8 The effect of temperature on the shear viscosity of different BSP systems (pH = 10).

4.4 High-pressure rheology measurements

In addition to the shearing effect, researchers have found that downhole pressure has a significant effect on the viscosity of borate-crosslinked fracturing fluids, which can be more than 80% lower than when measured at low pressure.[48–50] High-pressure rheology measurements of the BSP (0.5% BS + 0.5% CG) system (pH = 10) were carried out at 65 °C at a shear rate of 170 s^{-1}. The experimental procedure was as follows: shearing for 5 min under a certain pressure, where the experimental pressures used were 0.1, 15, 30, 45, 30, 15 and 0.1 MPa,

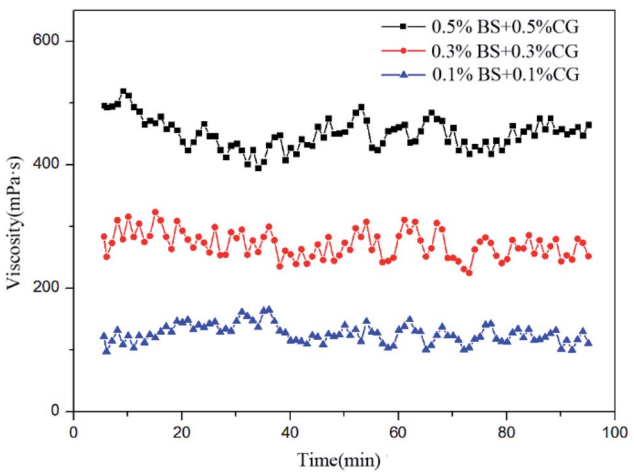

Fig. 9 The shear viscosity of BSP systems (pH = 10) at 65 °C, 170 s^{-1}.

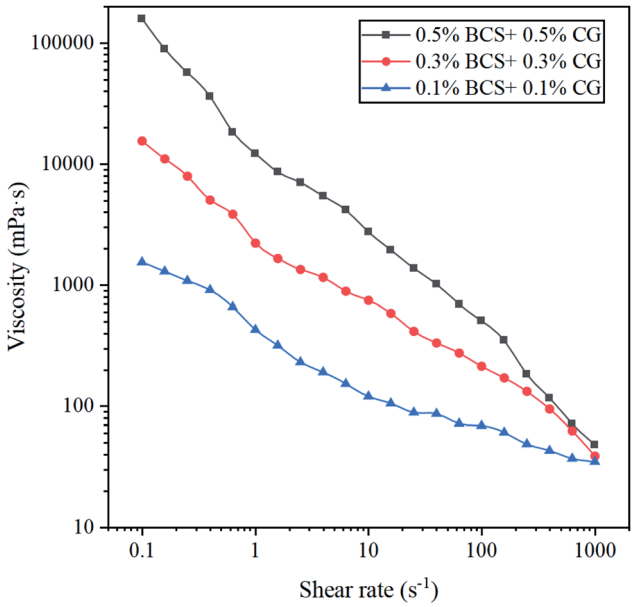

Fig. 10 Viscosity *vs.* the shear rate for the BSP systems (pH = 10) at 65 °C.

respectively. The experimental results are shown in Fig. 12, where it can be seen that the viscosities obtained by shearing at the seven different pressures are 478, 396, 311, 217, 294, 345 and 460 mPa s. This shows that for the BSP fracturing fluid, viscosity was rapidly lost with increasing pressure, and regained quickly when the pressure was reduced. The results show that pressure is the main factor that affects the viscosity of the fracturing fluid. Compared with a boron cross-linked fracturing fluid, the pressure has less effect on the viscosity loss of BSP.

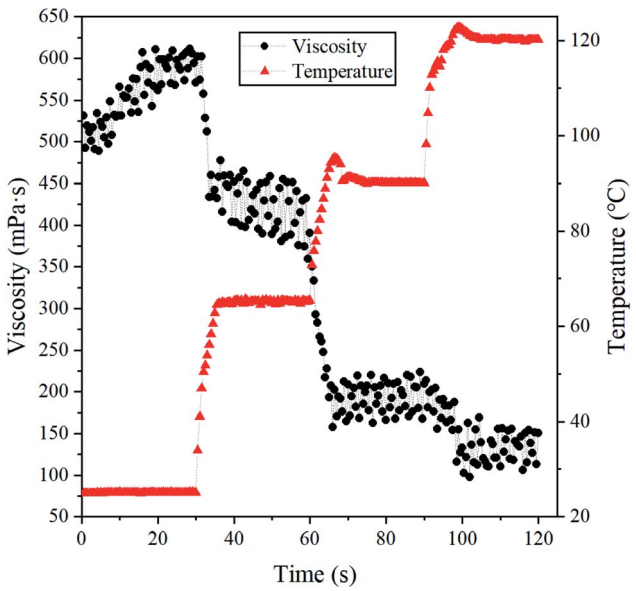

Fig. 11 The change in the shear viscosities of BSP (0.5% BS + 0.5% CG, pH = 10) systems according to temperature, at a shearing rate of 170 s^{-1}.

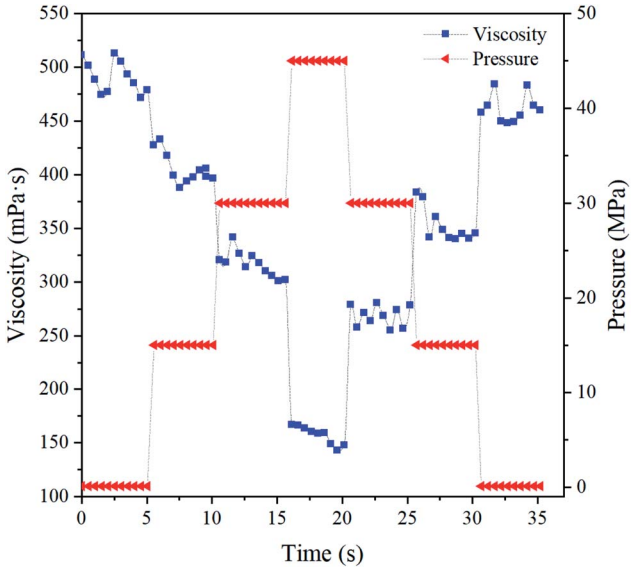

Fig. 12 High-pressure rheology testing of the BSP (0.5% BS + 0.5% CG) system (pH = 10) at 65 °C at a shear rate of 170 s^{-1}.

4.5 Shear recovery of the BSP

As a key parameter of a fracturing fluid, the shear rheology is used to judge the sand carrying capacity of a fracturing fluid and reduce the fracturing fluid loss.[39,41] It is used to judge the effect of maintaining the viscosity of the sheared fracturing fluid, but cannot be used to judge whether the viscosity of the sheared fracturing fluid can be restored. Taking Zr or Ti crosslinked gel fracturing fluids as an example,[51,52] the shear may destroy the network structure, making it impossible to regain the original viscosity. During the fracturing process, if the viscosity of a shear-treated fracturing fluid is able to be very well restored, it will achieve excellent depressing filter loss capacity again.

Shear recovery testing of the BSP (0.5% BS + 0.5% CG) system (pH = 10) was carried out at 65 °C. The experimental procedure was as follows: shearing for 5 min, allowing to stand for 5 min, and then shearing again for 5 min at shear rates of 20, 70, 120

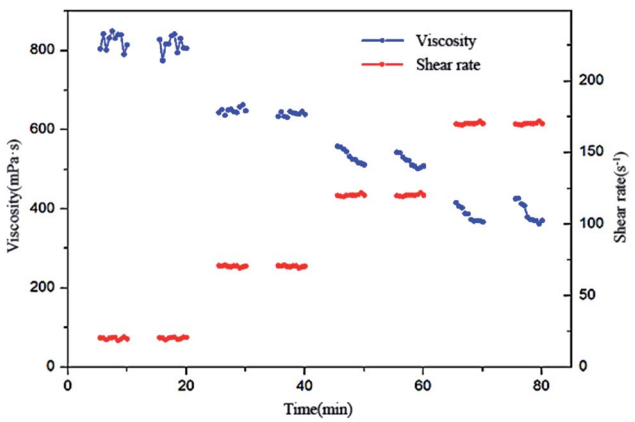

Fig. 13 Shear recovery testing of the BSP (0.5% BS + 0.5% CG) system (pH = 10) at 65 °C.

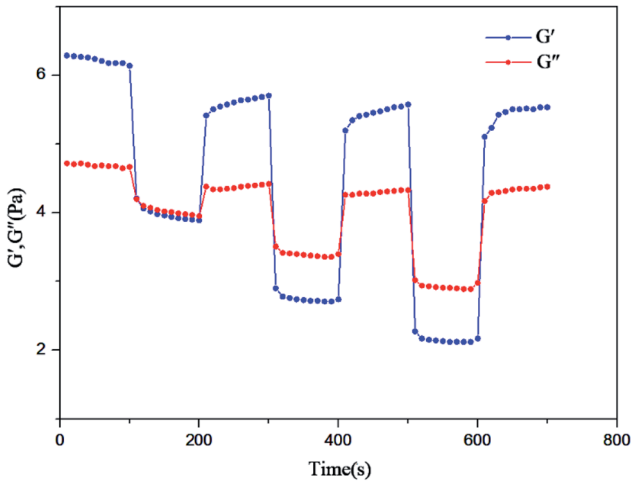

Fig. 14 Strain recovery testing of the BSP (0.5% BS + 0.5% CG) system (pH = 10) at 65 °C.

and 170 s^{-1}, respectively. According to the results of shear recovery testing (Fig. 13), it can be observed that the viscosities obtained by shearing twice at 20 s^{-1} are 813 and 805 mPa s, at 70 s^{-1} they are 647 and 638 mPa s, at 120 s^{-1} they are 511 and 508 mPa s and at 170 s^{-1} they are 367 and 371 mPa s. The results show that the viscosity of the BSP system can be almost completely restored during each shear cycling process, which indicates that the viscosity of the BSP system has self-repairing properties, meaning that the fracturing fluid does not lose any efficacy due to sand-carrying shear.

In order to test the influences of strain on the viscoelasticity of the fracturing fluid and recovery effect, the storage modulus G' and the loss modulus G'' of the BSP (0.5% BS + 0.5 CG) system (pH = 10, 65 °C) were tested under different strain ratios. The fluid was tested using a cone-plate test system for stress-scanning under the conditions of 1 Hz, and the shear stresses

Fig. 15 Images of the proppant suspension, (a) before settling at 25 °C and (b) after settling at 65 °C over 3 h.

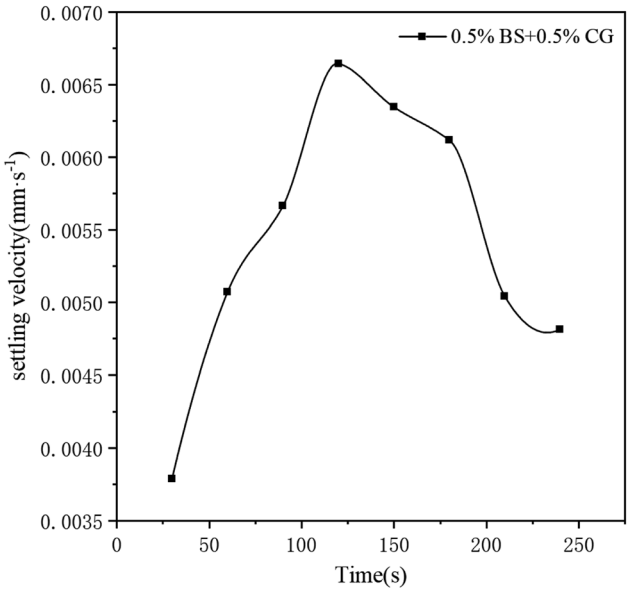

Fig. 16 Settling velocity of the BSP (0.5% BS + 0.5% CG, pH = 10) fracturing fluid with 30% of proppant at 65 °C.

in the yield stress scale sequence were set to: 1%, 100%, 1%, 200%, 1%, 300%, 1%, recording the modulus every 10 s. The experimental results are shown in Fig. 14.

When the yield stress is 1%, the storage modulus G' (6.14 Pa) is higher than the loss modulus G'' (4.67 Pa). Here, the fluid presents elastic fluid characteristics. With an increase in the shear stress, the storage modulus G' and the loss modulus G'' decrease gradually, with the storage modulus G' decreasing faster compared to the loss modulus G''. When the shear stress is equal to 200% of the yield stress, the loss modulus G'' (3.4 Pa) is higher than the storage modulus G' (2.74 Pa), and the fluid

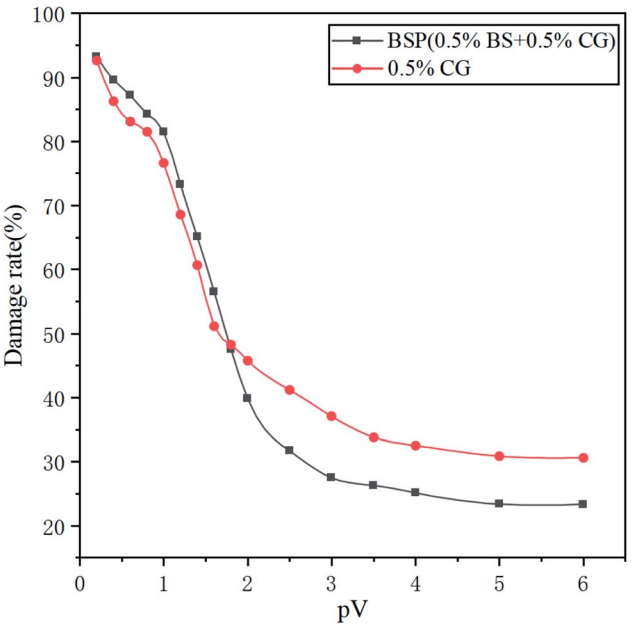

Fig. 17 Fracturing fluid damage comparison.

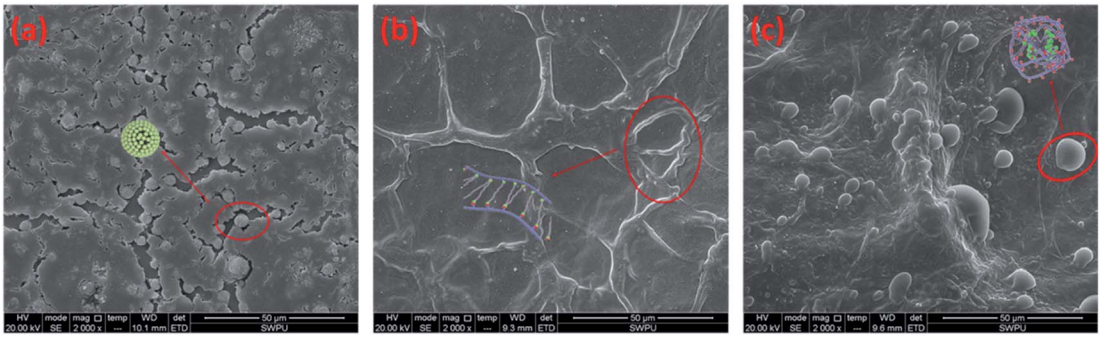

Fig. 18 SEM images of the (a) BS solution, (b) BSP solution (pH = 10), and (c) BSP solution (pH = 7).

shows the behavior of a viscous fluid. When the shear stress is 300% of the yield stress, it shows the same properties. However, when the shear stress is restored to 1%, the results (G', G'') are (5.71, 4.42), (5.58, 4.33) and (5.54, 4.38), respectively, after 100%, 200% and 300% yield stress. Therefore, it can be concluded that after shearing, the BSP system can be repaired and that shearing does not damage the network structure, as a result of the dynamic cross-linking effect of the electrostatic and hydrophobic interactions between BS and GC. In the process of fracturing, the BSP system can repair its network structure voluntarily to maintain viscosity after shearing caused by sand-carrying and rock formation, with no permanent network destruction.

4.6 Proppant suspension measurements

Suspension ability is an important property of a fracturing fluid. A fracturing fluid with good suspension properties is an effective way to ensure transport of a proppant to a fracture formation, and achieve high conductivity.[53–55] Fig. 15 shows the results of static proppant suspension tests, where BSP (0.5% BS + 0.5% CG, pH = 10) fracturing fluid with 30% of proppant was poured into a 100 mL in a measuring cylinder, and then heated to 65 °C, and Fig. 16 shows the settling velocity of the BSP (0.5% BS + 0.5% CG, pH = 10) fracturing fluid with 30% of proppant at 65 °C. The maximum settling velocity reached at 120 min was 0.0066 mm s^{-1}, reflecting the good proppant suspension capability of the BSP fracturing fluid.

4.7 BSP fracturing fluid damage characteristics

BSP fracturing fluid damage tests were carried out following the *SYT5107-2005 Water-Based Fracturing Fluid Evaluation Standard*[54] method with an artificial core permeability of 30 mD. During the initial state, the permeability, K_1, of the brine (2.0% KCl + 5.5% NaCl + 0.45% $MgCl_2$ + 0.55% $CaCl_2$) injected core was tested. The fracturing fluid was then injected into the core, then replaced with filtrate after 36 minutes, and then left for 2 h. Finally, the permeability, K_2, of the brine injected core was measured, and recorded over time. Fig. 17 shows the effect of PV (PV is a multiple of the pore volume of the core) on the damage rate. The results of the formation damage tests indicate that the damage rate of the BSP (0.5% BS + 0.5% CG) fracturing fluid is 23.3%, and for the 0.5% CG fluid it is 30.6%, showing that the bola surfactant can reduce the damage of reservoir permeability caused by guar gum.

4.8 Microstructure of the BSP

The microstructures of the BSP fracturing fluid and BS solution were investigated, and the results are presented in Fig. 18. Many supramolecular sphere structures can be observed in the BS solution, indicating that the bola-type surfactant has a strong tendency to aggregate, as shown in Fig. 18(a). The electrostatic interactions on the spherical surfaces of the BS only allow the formation of a dispersed state, which is different from a VES fracturing fluid, which depends on the hydrophobic action of surfactants to aggregate into a super micelle network, bringing about an improvement in the viscosity.[12,42,56] The supramolecular spheres assembled by the bola-type surfactant are beneficial for the low damage of the reservoir permeability of the fracturing fluid. Fig. 18(b) shows that at pH = 10, the network structure of the BSP fracturing fluid is formed by electrostatic bridges between CG and BS, contributing towards the improved viscosity of the fracturing fluid, which is beneficial for improving the elasticity and reducing filtration during the fracturing process.[40,57,58] With a decrease in the pH, the bola carboxylate surfactant gradually changes to a bola nonionic surfactant, and the hydrophobicity becomes greater than the hydrophilicity[59–61] at this time, leading to the destruction of the network structure of the BSP fracturing fluid. This entangles bola spheres with cationic guar chains, decreasing the viscosity of the BSP fracturing fluid, as shown in Fig. 18(c), which is conducive to the flow-back of the BSP and a reduction in reservoir damage.

5 Conclusions

A bola-type surfactant was synthesized using a simple method, and a BSP fracturing fluid system was prepared using the bola surfactant and cationic guar gum. The fracturing fluid shows a change in viscosity based on pH response and viscosity self-repairing capability after shearing. Therefore, it can be seen that such an excellent fracturing fluid could be considered to be used for low permeability impairment fractures in the future. Meanwhile, based on a series of experiments, six conclusions could be drawn. (1) The viscosity of the BSP system is the

highest at pH = 9–11, where the system is in the form of a gel network due to the electrostatic interactions between the two heads of the bola surfactant and the cationic guar gum, while when the pH is less than 7, it becomes a low-viscosity fluid. With a decrease in the pH, the electrostatic interactions weaken, causing the bola to self-assemble into supramolecular microspheres, attracting and wrapping the cationic guar gum chains. (2) The concentration of CG is the dominant factor affecting the viscosity of the BSP fracturing fluid. Bola acts as a bridging agent, and when the concentration ratio of CG to BS is 1 : 1, the viscosity increasing effect of the fracturing fluid is the best, when the reservoir pressure is lower than 45 MPa, BSP can be preferably composed of 0.5% BS + 0.5% CG or lower. (3) Rheological studies suggest that the viscosities of the BSP fracturing fluid show a sudden increase from 55 to 70 °C. (4) The investigated BSP systems are non-Newtonian fluids. Rheology and strain recovery measurements show that the BSP systems can be repaired and that the network structure cannot be destroyed by shearing at a shear rate of 170 s^{-1} and the shear stress equals 300% of the yield stress. (5) The BSP fracturing fluid shows good proppant suspension capability, and the maximum settling velocity of BSP (0.5% BS + 0.5% CG, 65 °C) with 30% of proppant was 0.0066 mm s^{-1} at 120 min. (6) The BSP fracturing fluid can reduce the damage to reservoir permeability compared with guar gum fracturing fluid. The damage rate of the BSP (0.5% BS + 0.5% CG) system is 23.3% and that of 0.5% CG fluid is 30.6%.

Conflicts of interest

There are no conflicts to declare.

Acknowledgements

This work was supported by the Open Fund (2016ZX05058-003) for high efficiency oil production engineering and supporting technology demonstration in the Bohai Oilfield.

References

1 P. Luo, W. G. Luo and S. Li, *Fuel*, 2017, **208**, 626.
2 J. Wang, H. Q. Liu, G. B. Qian, Y. C. Peng and Y. Gao, *Fuel*, 2019, **236**, 755–768.
3 B. Fu, Z. X. Ma, W. F. Zhang, Q. Zhang and L. F. Zhou, *IFEDC*, 2019, pp. 539–549.
4 X. Qin, S. Q. Yang, X. C. Hu, W. X. Song, J. W. Cai and B. Z. Zhou, *Fuel*, 2019, **239**, 429–436.
5 S. D. Golding, V. Rudolph and R. M. Flores, *Int. J. Coal Geol.*, 2010, **82**, 133–134.
6 Z. D. Liu, Y. P. Cheng, Y. K. Wang, L. Wang and W. Li, *Fuel*, 2019, **236**, 709–716.
7 B. L. Li, Y. L. Su, X. W. Li, W. D. Wang, M. M. Husein and R. Aguilera, *Fuel*, 2019, **239**, 587–600.
8 L. N. Xue and B. Chen, *Atlantis Press*, 2016, **67**, 575–578.
9 T. Lu, S. Liu and Z. Li, *Fuel*, 2019, **237**, 283–297.
10 J. C. Mao, X. J. Yang, Y. N. Chen, Z. Y. Zhang, C. Zhang, B. Yang and J. Z. Zhao, *J. Pet. Sci. Eng.*, 2018, **164**, 189–195.
11 J. Zhao, B. Yang, J. Mao, Y. Zhang and Y. Shao, *Energy Fuels*, 2018, **32**, 3039–3051.
12 W. F. Pu, D. J. Du and R. Liu, *J. Pet. Sci. Eng.*, 2018, **167**, 568–576.
13 S. B. Jang and B. H. Chon, *Geosyst. Eng.*, 2014, **17**, 150–156.
14 V. C. Santanna, F. D. S. Curbelo, T. N. C. Dantas, A. A. D. Neto, H. S. Albuquerque and A. I. C. Garnica, *J. Pet. Sci. Eng.*, 2009, **66**, 117–120.
15 A. Das, G. Chauhan, A. Verma, P. Kalita and K. Ojha, *J. Pet. Sci. Eng.*, 2018, **167**, 559–567.
16 D. Liu, M. Fan, L. Yao, X. Zhao and Y. Wang, *J. Pet. Sci. Eng.*, 2010, **73**, 267–271.
17 H. Li, H. Yang, Y. Xie, H. Li and P. He, *Chin. J. Chem. Phys.*, 2010, **23**, 491–496.
18 E. Grzadka and J. Matusiak, *Carbohydr. Polym.*, 2017, **175**, 192–198.
19 T. Lane, J. L. Holloway, A. H. Milani, J. M. Saunders, A. J. Freemont and B. R. Saunders, *Soft Matter*, 2013, **9**, 7934–7941.
20 M. S. Kamal, M. Mohammed, M. Mahmoud and S. Elkatatny, *Energies*, 2018, **11**, 1663.
21 Q. Jiang, G. Jiang, C. Wang, L. Yang, Y. Ren and P. Liu, *J. Nat. Gas Sci. Eng.*, 2016, **35**, 1207–1215.
22 G. Jiang, Q. Jiang, Y. Sun, P. Liu, Z. Zhang and X. Ni, *Energy Fuels*, 2017, **31**, 4780–4790.
23 A. Chandler, *Nature*, 2005, **437**, 640–647.
24 K. Jasleen and K. Gurpreet, *Polym. Adv. Technol.*, 2018, **29**, 3035–3048.
25 S. Wang, H. Tang, J. Guo and K. Wang, *Carbohydr. Polym.*, 2016, **147**, 455–463.
26 W. Chen, *Beijng Science Press*, 1984, 45–48.
27 D. W. VanKrevelen, *Properties of polymers, their correlation with chemical structure*, Elsevier, Amsterdam, 1990.
28 Y. Xu, *Chengdu Sichuan Education Press*, 1990, 136–139.
29 N. V. Thampi, R. P. John, K. Ojha and U. G. Nair, *Ind. Eng. Chem. Res.*, 2016, **55**, 5805–5816.
30 S. Kumar, P. Panigrahi, R. K. Saw and A. Mandal, *Energy Fuels*, 2016, **30**, 2846–2857.
31 H. Li, H. Yang, Y. Xie, H. Li and P. He, *Chin. J. Chem. Phys.*, 2010, **23**, 491–496.
32 S. R. Raghavan, G. Fritz and E. W. Kaler, *Langmuir*, 2002, **18**, 3797–3803.
33 Z. Yan, C. Dai, M. Zhao, Y. Sun and G. Zhao, *J. Ind. Eng. Chem.*, 2016, **37**, 115–122.
34 W. F. Pu, D. J. Du and R. Liu, *J. Pet. Sci. Eng.*, 2018, **167**, 568–576.
35 A. Das, G. Chauhan, A. Verma, P. Kalita and K. Ojha, *J. Pet. Sci. Eng.*, 2018, **167**, 559–567.
36 D. X. Liu, M. F. Fan, L. T. Yao, X. T. Zhao and Y. L. Wang, *J. Pet. Sci. Eng.*, 2010, **73**, 3–4.
37 M. B. Dowling, J. H. Lee and S. R. Raghavan, *Langmuir*, 2009, **25**, 8519–8525.
38 M. T. Popescu, S. Mourtas, G. Pampalakis, S. G. Antimisiaris and C. Tsitsilianis, *Biomacromolecules*, 2011, **12**, 3023–3030.
39 J. Mao, H. Zhang, W. Zhang, J. Fan, C. Zhang and J. Zhao, *J. Ind. Eng. Chem.*, 2017, **60**, 133–142.

40 Y. Zhang, C. Dai, Y. Qian, X. Fan, J. Jiang, Y. Wu, X. Wu, Y. Huang and M. Zhao, *Colloids Surf., A*, 2018, **553**, 244–252.
41 X. Wu, Y. Zhang, X. Sun, Y. Huang, C. Dai and M. Zhao, *Fuel*, 2017, **229**, 79–87.
42 Y. Zhang, J. Mao, J. Zhao, X. Yang, Z. Zhang, B. Yang, W. Zhang and H. Zhang, *Chem. Eng. J.*, 2018, **54**, 913–921.
43 J. Zhao, B. Yang, J. Mao, Y. Zhang and Y. Shao, *Energy Fuels*, 2018, **32**, 3039–3051.
44 N. V. Thampi, R. P. John, K. Ojha and U. G. Nair, *Ind. Eng. Chem. Res.*, 2016, **55**, 5805–5816.
45 U. Teipel, L. Heymann and N. Aksel, *Colloids Surf.*, 2001, **193**, 35–49.
46 J. Z. Zhao, B. Yang, J. C. Mao, Y. Zhang, X. J. Yang, Z. Y. Zhang and Y. Shao, *Energy Fuels*, 2018, **32**, 3039–3051.
47 S. M. Yan, Y. J. Wang, J. He and H. D. Zhang, *Russ. J. Appl. Chem.*, 2015, **88**, 1884–1891.
48 M. Marquez, N. Tonmukayakul, L. A. Schafer, M. B. Zielinski, P. Lord and T. L. Goosen, *High Pressure Testing of Borate Crosslinked Fracturing Fluids, SPE-152593-MS*, 2012.
49 M. D. Parris, B. A. MacKay, J. W. Rathke, R. J. Klingler and R. E. Gerald, *Macromolecules*, 2008, **41**, 8181–8186.
50 A. Wilson, *J. Pet. Technol.*, 2017, **69**, 48–51.
51 G. Chauhan, A. Verma, A. Doley and K. Ojha, *J. Pet. Sci. Eng.*, 2019, **172**, 327–339.
52 T. Hurnaus and J. Plank, *Energy Fuels*, 2015, **29**, 3601–3608.
53 J. C. Mao, H. Zhang, W. L. Zhang, J. M. Fan, C. Zhang and J. Z. Zhao, *J. Ind. Eng. Chem.*, 2018, **60**, 133–142.
54 J. C. Zhang, K. Y. Liu and M. Cao, *Fuel*, 2017, **199**, 185–190.
55 A. M. Gomaa, D. V. S. Gupta and P. Carman, *Viscoelastic Behavior and Proppant Transport Properties of a New High-Temperature Viscoelastic Surfactant-Based Fracturing Fluid, SPE-173745-MS*, 2015.
56 J. Mao, X. Yang, D. Wang, Y. Li and J. Zhao, *RSC Adv.*, 2016, **6**, 88426–88432.
57 G. Chauhan, A. Verma, A. Hazarika and K. Ojha, *J. Taiwan Inst. Chem. Eng.*, 2017, **80**, 978–988.
58 X. Zhao, J. Guo, H. Peng, R. Pan, A. O. Aliu, Q. Lu and J. Yang, *J. Nat. Gas Sci. Eng.*, 2017, **43**, 179–189.
59 H. Lu, Q. Shi, B. Wang and Z. Huang, *Colloids Surf., A*, 2016, **494**, 74–80.
60 Z. Zhai, X. Yan, J. Xu, Z. Song, S. Shang and X. Rao, *Chem. Commun.*, 2018, **54**, 12171–12173.
61 K. Liu, J. Jiang, Z. Cui and B. P. Binks, *Langmuir*, 2017, **33**, 2296–2305.